

11. OKT. 1977

Internal Report
DESY F41-77/05
September 1977

Luminescence Properties of Rare Gas Solids

I. Emission Bands and Excitation Spectra

by

G. Zimmerer

II. Institut für Exp. Physik der Universität Hamburg

LUMINESCENCE PROPERTIES OF RARE GAS SOLIDS

I. EMISSION BANDS AND EXCITATION SPECTRA ⁺⁾

G. Zimmerer

II. Institut für Exp. Physik der Universität Hamburg

Luruper Chaussee 149, D-2000 Hamburg 50

I. INTRODUCTION

Since several years ago, rare gas solids (RGS) have attracted much interest because they are the simplest solids known to us (1). As purely Van der Waals bound crystals they are the model substances for the variety of molecular solids. In this respect they play a similar role to that of Si, Ge for solids with covalent bonds, the alkali metals for metallic binding and alkali halides for ionic crystals.

The electronic structure (2) as well as the crystal properties are an immediate consequence of the closed shell configuration of the valence electrons (Table 1). The ionization energies of free atoms and the band gaps of RGS are very large. The onset of absorption is governed by two spin-orbit split exciton series (Fig. 1). The exciton series are classified by the total angular momentum $j=3/2$ (main quantum number: n) and $j=1/2$ (main quantum number: n') of the holes. Excitons with $n, n' > 1, 1'$ are Wannier excitons. The members $n=1, n'=1'$ are localized to about one unit cell and therefore are more Frenkel-type excitons. Often they are attributed to the first ($n=1 \hat{=} {}^3P_1$) and second ($n'=1' \hat{=} {}^1P_1$) resonance line of the atom. The very large binding energies, the spin-orbit splitting, the energies of the $n=1, n'=1'$ excitons, the ionization limit of the $j=3/2$ series ($\hat{=} \text{band gap, } E_g$) are summarized in Table 1.

RGS solidify only at rather low temperature (Table 1). Under normal conditions they crystallize in a fcc lattice with one atom in the unit cell, and a large nearest neighbour distance (Table 1).

+)

to be published in "Luminescence of Inorganic Solids",
Proc. of the NATO Advanced Study Institute, Erice, Italy, 1977,
ed. by B. Di Bartolo and D. Pacheco, Plenum Press.

Optical phonons are absent. Acoustical phonons have small energies due to the weak binding (Table 1). These unique properties of the phonon spectra are important for an understanding of the luminescence and relaxation processes.

In contrast to the electronic structure and the crystal properties, luminescence of RGS is a rather young field. It was opened by Jortner et al. (3) in 1965. Since it became known that condensed rare gases are suited for vacuum ultraviolet (VUV) laser application (4) there was an exploding number of luminescence experiments (5). Besides the luminescence properties and the nature of the radiative states the radiationless processes between the creation of a high excited state of the crystal and the population of the radiative states are of particular interest.

Detailed information on luminescence as well as the radiationless processes are obtained under excitation with monochromatic light. Due to the lack of suitable light sources in the VUV, RGS were excited predominantly with α -particles, x-rays, and electrons. The references are listed in (5). Photoluminescence experiments were very scarce (6). A break-through was achieved when in 1974 for the first time monochromatized synchrotron radiation was used for exci-

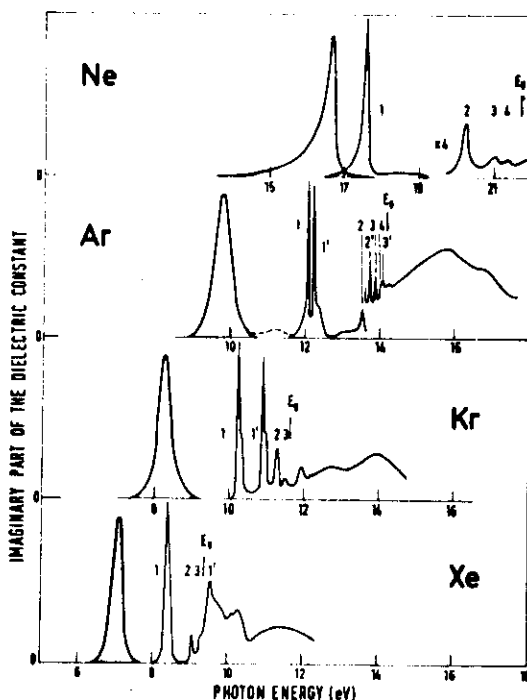


Fig. 1: ϵ_2 of solid Ne (5 K), Ar (10 K), Kr, and Xe (20 K) (2,5).
Shaded curves: photoluminescence of solid Ne (14), Ar, Kr, Xe (5) (5 K).

Table 1. Some basic data characterizing RGS (1,2,5)

	Ne	Ar	Kr	Xe
electronic configuration of free atoms	$2s^2 2p^6$	$3s^2 3p^6$	$4s^2 4p^6$	$5s^2 5p^6$
melting point (deg. K)	24.5	84.0	116.6	161.3
nearest neighbour distance fcc-lattice, 0 K (Å)	3.13	3.76	4.01	4.35
maximal phonon TA(X) energies (meV) LA(X)	4.5 7	6.2 8.3	4.15 6.2	3.7 5.4
ionization energy of free atoms (eV)	21.6	15.8	14.0	12.1
energies of $n=1$ excitons (eV) * $n'=1'$	17.59 17.79	12.06 12.24	10.17 10.86	8.37 9.51
band gap (eV)	21.69	14.16	11.61	9.33
binding energy of the $j=3/2$ exciton series (eV)	5.24	2.36	1.53	1.02
spin-orbit splitting (eV)	.1	.184	.688	1.3

* These data are taken from Ref. 8

tation purposes (7). Only with this light source was it possible to scan simultaneously both the excitation and luminescence wavelength over a large spectral range.

Luminescence experiments on RGS are not merely complicated by the fact that both the excitation and luminescence light are in the VUV. They also need low temperature and ultra-high vacuum techniques especially if surface sensitive excitation is used (e.g. photo excitation). A weak aspect of the investigations done so far is the fact that condensed films or bulk polycrystalline samples are used but no real single crystals. In situ preparation of single crystals would mean another very hard requirement for the experiments.

Luminescence experiments on solid He have not been done so far because He only solidifies under pressure (26 atm). Therefore He is not discussed in this contribution.

II. EMISSION BANDS OF PURE RARE GAS SOLIDS

The emission bands of RGS are due to pure samples. They are not due to the unperturbed, ideal lattice but stem from a luminescence centre which is created after excitation and disappears after the luminescence process. RGS show broad band ordinary luminescence (OL) dominating in Xe, Kr, Ar, broad band hot luminescence (HL) established so far in Ar, Ne, and narrow line luminescence (Xe, Kr, Ar, Ne) dominating in Ne.

II.A. The Main Luminescence Bands of Xe, Kr, Ar (OL)

Fig. 2 and Fig. 1 show the dominant RGS luminescence bands. Solid Xe, Kr, Ar yield broad, Stokes-shifted bands. The energies, widths and Stokes shifts are summarized in Table 2. The Stokes shifts are illustrated in Fig. 1. An exciting feature of Xe, Kr, Ar luminescence is its close similarity to the luminescence of the liquid and the dense gaseous phase (pressure \approx 1000 Torr) (3). The Xe, Kr, Ar bands of Fig. 2 have been obtained under optical excitation (5). They are independent of the energy of optical excitation as well as of the kind of excitation. They are natural candidates for VUV lasers (mainly in the dense gaseous phase (9)). The energetic position somewhat depends on sample preparation and annealing conditions (10). With increasing temperatures they shift slightly to lower energies (10, 11).

II.B. Luminescence of Solid Ne

Ne obviously behaves differently from Xe, Kr, Ar. Its luminescence (Fig. 2) consists of a rather sharp band (16.7 eV) with a Stokes

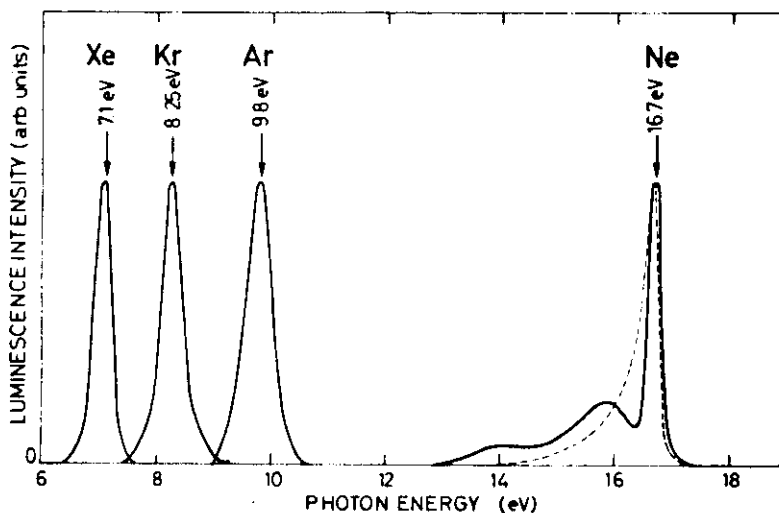


Fig. 2 The main luminescence bands of RGS (5K). The Xe, Kr, Ar and dotted Ne curves: optical excitation (5,14). Full Ne curve: x-ray excitation (13)

shift of less than 1 eV. This band shows splitting into sharp components (see II.C.). At the low energy side two broad bands are found at ~ 14 eV and ~ 16 eV under electron (12) and x-ray excitation (13). Optical excitation (14) results only in a low energy tail extending down to less than 14 eV. The 14 eV and 16 eV band are hot luminescence and no OL band similar to the bands of Xe, Kr, Ar exists (Sec. III).

II.C. Hot Luminescence and Narrow Line Luminescence

Fig. 3 shows luminescence spectra of Xe (15), Kr (16), Ar (11) found between the OL-bands and $n=1$ exciton absorption. The integrated intensities of these weak bands are three to four orders of magnitude smaller than the intensities of the OL bands. For comparison a high resolution analysis of the 16.7 eV Ne band (13) is added. Note, however, that for Ne this is the main contribution to luminescence. In all cases, narrow line luminescence is found which is only slightly Stokes shifted compared to $n=1$ exciton absorption (Table 2). The emission lines nearly coincide with the lowest levels (included in Fig. 3) of the free atoms. For Ar at the low energy side of the narrow lines, a broad asymmetric band (11.37 eV) has been well established (11). It corresponds to the 16 eV Ne HL band. The weak 9.69 eV Kr band may also be a HL band but this is not established so far. In

Table 2. Luminescence bands of RGS

	Xe	Kr	Ar	Ne
energy of broad band ordinary luminescence (eV)	7.1	8.25	9.8	-
fwhm of the OL bands (eV)	.4	.45	.55	-
Stokes shift of OL (eV)	1.3	1.9	2.3	-
energy of broad band hot luminescence (eV)	?	9.69 ?	11.37	14 16.1
narrow line luminescence (eV)	8.18 8.33	9.92 10.12	11.59 11.64	16.66 16.71 16.8 16.9
Stokes shift of narrow line luminescence (eV) [§]	.19	.25	.47	.93

[§] difference between energy of $n=1$ excitons in absorption (Table 1) and the low energy component of narrow line luminescence.

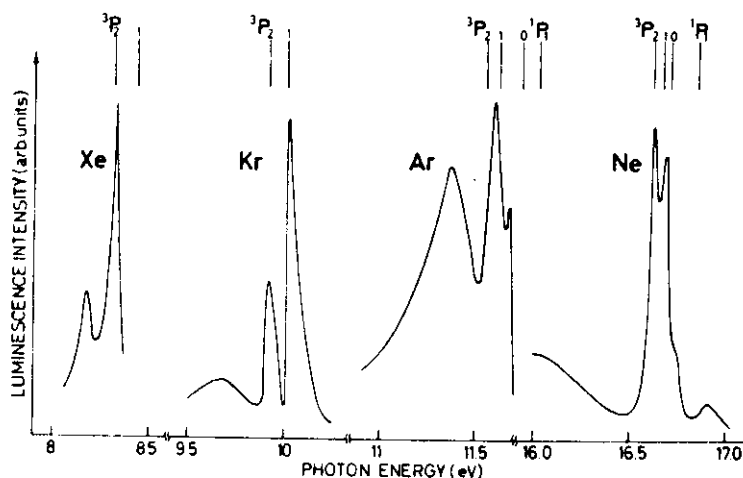


Fig. 3 Narrow line and hot luminescence of Xe, 4K-60K (15), Kr, 40K (16), Ar, 4.5K (11), Ne, 11K (13). For comparison purposes, the energies of the lowest excited atomic states are indicated.

Xe, an analogous band has not so far been found. The results on Kr (16) and Ar (11) indicate that the relative intensities of the features of Fig. 3 depend somewhat on temperature. In general, there is an increasing tendency for narrow line luminescence as well as HL when progressing from Xe to Ne.

III. THE LUMINESCENCE CENTRES AND EXPLANATION OF THE LUMINESCENCE SPECTRA

III.A. Formation and Properties of the Molecular Centre, R_2^*

From the close similarity of the main luminescence bands of Xe, Kr, Ar in the condensed and gaseous phases, Jortner et al. (3) already concluded that the centre responsible for these bands is the diatomic rare gas molecule, R_2^* (R stands for any kind of rare gas atom). In the gas phase, these molecules are well established (excimers). They have a strongly repulsive ground state (apart from a shallow Van der Waals minimum at large internuclear distances). The lowest excited electronic states are bound and stem from the excited atoms $R^*(^3P_2)$ and $R^*(^3P_1)$ and ground state atoms $R(^1S_0)$. The neutral, bound R_2^* molecules can also be regarded as molecules consisting of the well known molecular ion, R_2^+ , as a core, and an electron occupying a Rydberg orbital of the R_2^+ . The molecular states have been treated theoretically by Mulliken (\bar{Xe}) (17), Lorents and Olson (18) (Ar) in a phenomenological way. Ab initio calculations exist for Ne_2^+ (19).

In the solid, the molecule acts like an impurity in a matrix of the same kind of atoms for the following reason. The equilibrium distance ($\text{Ne}_2^* \sim 2 \text{ \AA}$ (19), $\text{Ar}_2^* \sim 2.5 \text{ \AA}$ (18), $\text{Kr}_2^* \sim 2.8 \text{ \AA}$ (20), $\text{Xe}_2^* \sim 3.3 \text{ \AA}$ (17)) of the molecule is much smaller than the nearest neighbour distance in the unperturbed lattice (Table 1). With an internuclear distance reaching the value of the nearest neighbour distance of the lattice, the molecule already dissociate.

The molecular centres are only created after electronic excitation in two different ways:

(i) Starting from an excitonic excitation, excitons are self-trapped in the lattice. Excitons can migrate in the crystals via resonant transfer between nearest neighbours. In each transfer step both the atoms involved can be regarded as a molecule near the dissociation limit in a very high vibrational state. Via coupling to the lattice phonons it is possible to transfer some vibrational energy to the lattice during a resonant transfer of the exciton. After such a conversion of (local) vibrational energy into lattice phonons the energetic resonance with other nearest neighbours is destroyed: the free exciton is then self-trapped (21). The self-trapped exciton (STE) is nothing else than the R_2^* molecule. Because in an fcc lattice the nearest neighbours are found in the 110-direction, the molecular axis is aligned to a 110-direction.

(ii) Starting from a free electron-hole pair (band to band excitation), it is well known from transport properties (22) that the holes are self-trapped similarly to the excitons. The self-trapped holes (STH) can be regarded as molecular ions, R_2^+ . Calculations of the STH-properties confirm the intuitively assumed geometrical alignment along the 110-direction and show that the lattice around the centre is affected only very little (23,24). The STH can capture a slow free electron (from the bottom of the conduction band) resulting in the $\text{STE} \hat{=} \text{R}_2^*$.

The influence of the surrounding lattice comes into play in the following processes which are discussed in more detail in part II (25), together with the time hierarchies involved.

- (i) Vibrational relaxation of the molecular centre via coupling of local modes to the phonon bath of the crystal.
- (ii) Splitting of the states of the free molecule and modification of oscillator strengths by the crystal field.

III.B. Radiative Decay of the Molecular Centre

The potential curves of the centre are sketched in Fig. 4. The internuclear distance of the molecule acts as configurational coordinate. Immediately after formation, the centre is vibrationally excited. Vibrational relaxation competes with radiative decay. The

spacing of vibrational levels increases going from Xe to Ne. Due to the low phonon energies, multi-phonon processes are required for vibrational relaxation. Whereas the order of multi-phonon processes is small in Xe and only slightly increases via Kr to Ar, there is a dramatic jump from Ar to Ne (numerical values given in part II (25)). This is the reason for the different luminescence behaviour of Xe, Kr, Ar on the one hand and Ne on the other.

In Xe, Kr, Ar, thermal equilibrium is obtained before radiative decay. The main luminescence bands stem from the vibrationally relaxed molecule and terminate in the repulsive part of the ground state. The Stokes shift is composed of (i) the depth of the excited state potential curve (~ 5 eV (Xe) up to ~ 1 eV (Ar)) and the height of the ground state potential curve. The width of the luminescence bands simply reflects the slope of the ground state.

In Ne fast vibrational relaxation starts in the anharmonic part of the potential but is slowed down dramatically reaching lower vibrational levels. Yakhot et al. (26) showed that relaxation sticks in the 3rd vibrational level which decays radiatively. They calculated the Franck-Condon factors for this transition using the ab initio potential curves for Ne (19). In Fig. 5, these results are compared with experiment. The broad 14 eV and 16 eV Ne lumi-

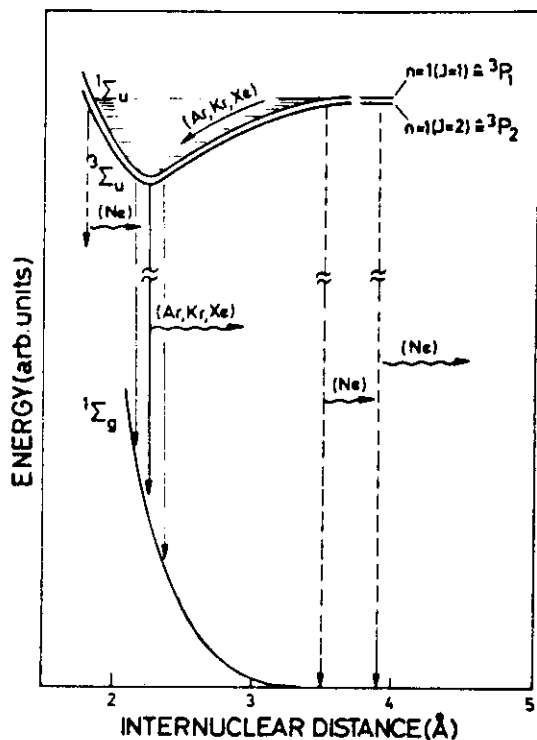


Fig. 4 Potential curves of the molecular centre (realistic for Ar_2^*). The main luminescence transitions are indicated schematically.

nescence bands are well reproduced. This proves that the Ne luminescence is hot luminescence except for the 16.7 eV band. Ne seems to be a prominent example in the field of HL.

The 11.37 band of Ar is also explained as HL starting from high vibrational levels of the Ar_2^* centre. Not only the calculation of vibrational relaxation rates (27) but also comparison with gas phase data lead us to this interpretation. In the gas phase, the relaxation rate can be slowed down continuously by decreasing gas pressure (28) and HL shows up. Depending on pressure, the maximum of HL is found between 11.6 eV and 11 eV. The 11.37 eV band nicely fits into this range.

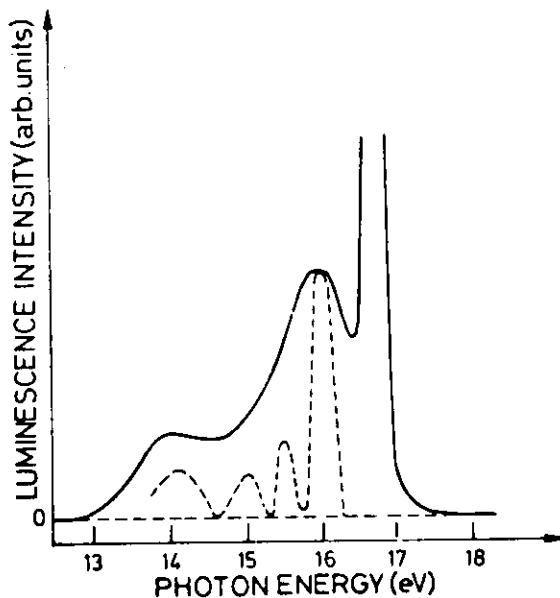


Fig. 5 Comparison between experiment (13) (full curve) and calculated hot luminescence spectrum of solid Ne (26)

III.C. Origin of the Narrow Luminescence Lines

A detailed understanding of the narrow luminescence lines has still to be achieved. Recently they have been ascribed to the decay of free excitons (15,29). For Kr and Xe, the very small Stokes shifts could be caused by reabsorption. The Stokes shifts of the Ar and Ne lines, however, indicate the existence of an atomic centre formed by a medium relaxation around a $n=1$ exciton (30). Due to this medium relaxation, the transition energies come very close to the free atom values. Tentatively the two components (see Fig. 3 and Table 2) may be ascribed to the decay of "atomic" 3P_2 and 3P_1 states to the 1S_0 ground state. The lower ($^3P_2 \rightarrow ^1S_0$) transition may become allowed through the influence of the crystal field. In Ne, spin-

orbit splitting is so small that all four components of the $3p^5 4s$ configuration may contribute to luminescence.

The relative intensity of the molecular emission and the narrow line emission seems to be controlled by a potential barrier between both centres (self-trapping barrier). In Xe and Kr this barrier seems to be very small. Values have been estimated for Ar (3meV) and Ne (10meV) (11). The relatively large Ne value seems to be responsible for the dominance of the narrow line luminescence.

IV. PHOTOLUMINESCENCE YIELD SPECTRA

Photoluminescence yield (PLY) spectroscopy is a special technique offered by photo-excitation. In a PLY experiment (often called excitation spectrum) we measure the quantum efficiency (in relative units) of a certain luminescence band as a function of the excitation energy. A PLY thus probes the processes which influence the population of the radiative state after excitation of an energetically selected excited state of the system.

IV.A. PLY for Excitonic Excitations

Here we are dealing with excitation energies covering the exciton series (Fig. 1). In Fig. 6, the PLY curves of the main luminescence bands of Xe (31), Kr (32), Ar (33) are shown. They show pronounced minima which coincide with the excitonic maxima of absorption. This is typical for samples with a surface covered with acceptor atoms. The quantum efficiency of samples with a clean surface (32) is nearly independent of excitation energy in the range covered by Fig. 6. The minima due to surface coverage indicate surface quenching of free excitons which reach the surface before self-trapping. Quenching is only effective if the excitons are created near to the surface (penetration depth of exciting light comparable with the diffusion length L).

In (32) it is shown that the PLY curve can be calculated taking into account exciton diffusion and "collision-induced" energy transfer from excitons to the acceptor atoms at the surface. Results of such calculations are shown in Fig. 6 (dotted curves). From a comparison between experimental and model curves, values for L of free excitons can be deduced: $150 \text{ \AA} - 1000 \text{ \AA}$ for Xe (L sensitively depends on annealing of the samples), $\sim 200 \text{ \AA}$ for Kr, and $40 \sim 80 \text{ \AA}$ for Ar. Thus PLY spectroscopy is well suited to the investigation of the exciton dynamics of RGS excitons.

In part II (25) it will be shown that L is not a constant but depends on excitation energy which follows for example from photoelectron emission measurements on RGS. There exist two PLY results up to now which point in the same direction.

(i) In (31) PLY spectra have been obtained from very thin samples ($d \sim 100 \text{ \AA}$) with a metal substrate (perfect quencher for excitons reaching the RGS/metal interface). For all excitation energies, luminescence was completely quenched with one exception: the maximum of the PLY spectrum at the low energy tail of the $n=1$ exciton persists. Obviously the diffusion length drops down dramatically in the low energy tail of the $n=1$ exciton to values far below 100 \AA (experiment only done for Xe). In Fig. 6, this range of energy is not covered by the model calculation because the absorption coefficient is not known well enough in the low energy tail of $n=1$ excitons. A precise knowledge of α is an essential ingredient for the model calculation.

(ii) The result on Ar (33) of Fig. 6 could only be fitted satisfactorily with a value of L increasing from $\sim 40 \text{ \AA}$ ($n=1$ exciton) to $\sim 80 \text{ \AA}$ ($n=2$ exciton).

The dependence of L on excitation energy must contain information on electronic relaxation from higher excitons to lower excitons. Quantitative results, however, need more precise measurements which should be made on single crystals.

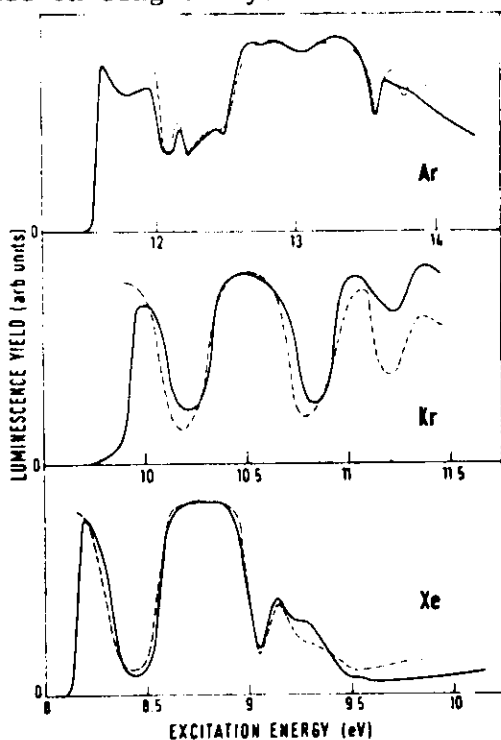


Fig. 6 PLY spectra of the 7.1 eV Xe, 8.25 eV Kr, and 9.8 eV Ar luminescence band at 5K. Dotted curves: model calculations.

IV.B PLY Spectra in the Range of Band-to-Band Transitions

With excitation energies larger than the band gap, free photoelectrons are created. If the initial kinetic energy is high enough, the photoelectrons can be scattered inelastically at valence electrons and additional excitations (excitons or electron-hole pairs) are created. In solid Ar (34), such scattering processes lead to a stepwise increase of the PLY curve (Fig. 7). Onset energies for the scattering processes of the form $E_g + m \cdot E_{ex}$ could be deduced, $m=1,2,3$ (E_{ex} : energy of $n=1$ excitons). Therefore at the onset of the steps the photoelectron is scattered to the bottom of the conduction band and excitons are created. The first step at an excitation energy $E_g + E_{ex} \sim 2 E_g$ is not contradictory to the situation in semiconductors (35) because the effective mass of valence holes is much larger than the electron mass (case $\mu=0$ in Autoncik's paper).

The result on Ar shows that the main contribution to relaxation of highly kinetic photoelectrons is due to inelastic electron-electron scattering. From a more general point of view it is interesting to note that the results seem to indicate creation of electronic polaron complexes (36) by the excitation process itself (34).

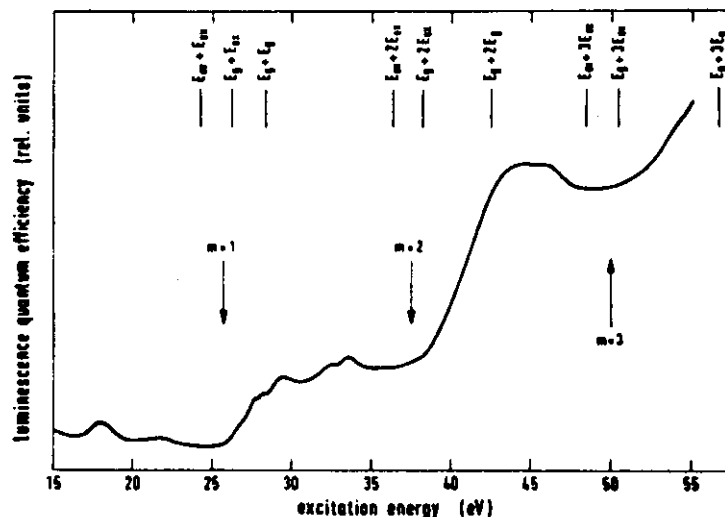


Fig. 7 PLY spectrum of the 9.8 eV Ar luminescence band at 5K (34)

V. LUMINESCENCE OF RGS WITH ISOELECTRONIC IMPURITIES

Isoelectronic impurities in RGS lead to a variety of luminescence features (10,11,37-40) which are important for the investigation of electronic multi-phonon relaxation, lattice relaxation, and energy transfer processes (30). Some of these aspects will be covered in part II (25). Here we only want to sketch some typical luminescence phenomena observed in RGS doped with isoelectronic impurities.

In these systems with increasing impurity concentration the host luminescence is quenched and different impurity bands show up. At low concentrations, the emission of isolated impurities X^* is found. It is Stokes shifted compared with impurity absorption but nearly coincides with the resonance lines of the free atoms. Both the 3P_1 and 1P_1 lines are established. Besides X^* emission, heteronuclear molecules RX^* (R: host atom) show up in luminescence. At larger concentrations, X_2^* molecules radiate and finally dominate.

The luminescence spectra not only depend on concentration but also on the excitation energy. This can only be probed with monochromatic photoexcitation. As an illustrative example, in Fig. 8 results on Ar doped with 3 % Kr are shown (39). In this system, all kinds of impurity emission exist: $Kr^* ^1P_1$ (I), $Kr^* ^3P_1$ (II), $ArKr^*$ (III,IV), Kr_2^* (VI). Curve a) was obtained under host excitation. Excitation of $Kr ^3P_1$ and $Kr ^1P_1$ in the Ar matrix leads to the luminescence spectra b) and c). In b), of course, the $Kr^* ^1P_1$ band is missing. In c) the $Kr^* ^1P_1$ band is much stronger than the 3P_1 band (intersystem crossing ineffective). Curve d) was excited with 10.2 eV photons. Both Kr^* bands are absent. The PLY of the $ArKr^*$ 9.88 eV band indicates that in the "transparency region" of the matrix a conti-

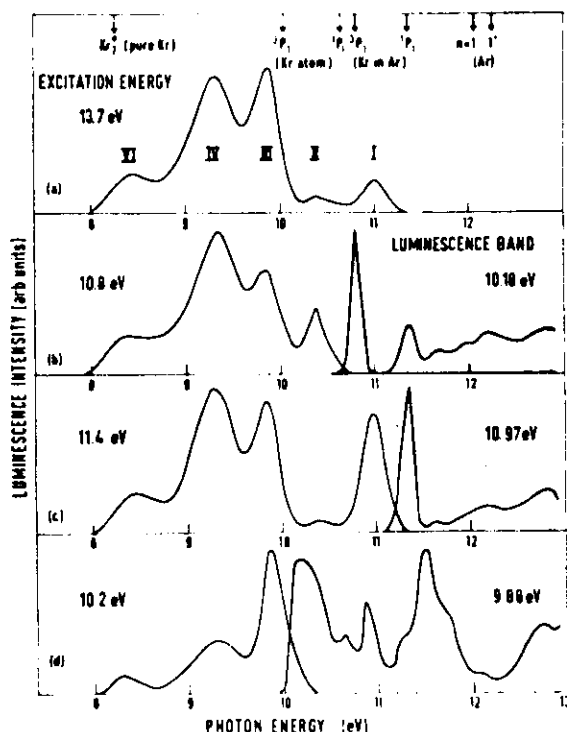


Fig. 8 Impurity luminescence of Kr doped Ar and PLYs (shaded curves) at 5K. Excitation energies for luminescence, and luminescence energies for PLYs are given in the figure. Resolution ~ 0.3 eV (luminescence) and ~ 0.05 eV (PLY curves).

nuous background of states exists perhaps due to molecular Ar-Kr interaction. The absorption of isolated Kr atoms is sorted out from this background in the PLYs of the Kr* luminescence bands (see b), c) of Fig. 8). The PLYs of energetically selected luminescence bands of samples with known thickness seem to be a measure for host-impurity interaction. More detailed investigations should enable us to discriminate between states of isolated impurities and host-impurity molecular states.

References

1. Rare Gas Solids, ed. by M.K. Klein and J.A. Venables, Academic Press, New York, London, Vol. I (1976), Vol. II (in press)
2. U. Rössler, in Rare Gas Solids I, loc.cit. p. 505 (theory)
B. Sonntag, in Rare Gas Solids II, loc.cit. chapter 19 (experiment)
3. J. Jortner, L. Meyer, S.A. Rice, and E.G. Wilson, *J.Chem. Phys.* 42, 4250 (1965)
4. N.G. Basov, *IEEE QE-2*, 354 (1966)
N.G. Basov, V.A. Danylichev, Yu.M. Popov, and D.D. Khodkevich *ZhETF Pis.Red.* 12, 473 (1970)
5. G. Zimmerer, in Proc. of the Internat. Summer School on Synchrotron Radiation Research (Alghero 1976), Vol. I, p. 433, ed. by A.N. Mancini and J.F. Quercia, Internat. College on Appl. Phys. Catania, and Int.Report DESY F41-76/10 (1976)
6. V.A. Danylichev, G.N. Kashnikov, Yu.M. Popov, Preprint No. 136 of the Lebedev Phys.Inst. Moscow (1970)
T. Nanba and N. Nagasawa, *J.Phys.Soc. Japan* 36, 1216 (1974)
N. Nagasawa and T. Nanba, *Opt.Comm.* 11, 152 (1974)
7. R. Brodmann, R. Haensel, U. Hahn, U. Nielsen, and G. Zimmerer, *Chem.Phys.Letters* 29, 250 (1974)
8. V. Saile, W. Steinmann, and E.E. Koch, private communication
V. Internat. Conf. on VUV Radiation Physics, Montpellier (France), September 1977
9. C.K. Rhodes, *IEEE QE-10*, 153 (1974)
10. A. Gedanken, B. Raz, and J. Jortner, *J.Chem.Phys.* 59, 5471 (1973)
11. I.Ya. Fugol, A.G. Belov, E.V. Savchenko, and Yu.B. Poltoratski, *FNT (USSR)* 1,2, 203 (1975); *Sov.J. Low Temp. Phys.* 1,2, 98 (1975)
12. R.E. Packard, F. Reif and C.M. Surko, *Phys.Rev.Lett.* 25, 1435 (1970)
13. E. Schuberth and M. Kreuzburg, *phys.stat.sol. (b)* 71, 797 (1975)
14. U. Hahn, B. Jordan, N. Schwentner, and G. Zimmerer, to be published
15. I.Ya. Fugol, A.G. Belov, Yu.B. Poltoratski, and E.V. Savchenko, *FNT (USSR)* 2, 400 (1976)
16. J. Hanus, F. Coletti, A.M. Bonnot, and J.M. Debever, in Vacuum Ultraviolet Radiation Physics, ed. by E.E. Koch, R. Haensel, and C. Kunz, Pergamon-Vieweg, Braunschweig 1974, p. 341

17. R.S. Mulliken, J.Chem.Phys. 52, 5170 (1970)
18. D.C. Lorents and R.E. Olson, Semiannual Technical Report no 1, Stanford Res. Inst. Menlo Park, California (1972)
19. J.S. Cohen and B. Schneider, J.Chem.Phys. 61, 3230 (1974)
20. R. Brodmann, thesis, University of Hamburg (1976)
21. M. Martin, J.Chem.Phys. 54, 3289 (1970)
22. P.G. Le Comber, R.J. Loveland, and W.E. Spear, Phys.Rev. B11, 3124 (1975)
23. S.D. Druger and R.S. Knox, J.Chem.Phys. 50, 3143 (1969)
24. K.S. Song, Can.J. of Physics 49, 26 (1971)
25. N. Schwentner, this volume
26. V. Yakhot, M. Berkowitz and R.B. Gerber, Chem.Phys. 10, 61 (1975)
27. V. Yakhot, Chem.Phys. 14, 441 (1976)
28. R. Brodmann and G. Zimmerer, J. Physics B (in press)
29. Y. Toyozawa, in Vacuum Ultraviolet Radiation Physics, loc.cit. p. 317
R. Brodmann, G. Tolkiehn, and G. Zimmerer, phys.stat.sol. (b) 73, K99 (1976)
E.I. Rashba, Izv.Akad. Nauk SSSR, Ser.Fiz. 40, 1793 (1976)
30. J. Jortner, in Vacuum Ultraviolet Radiation Physics, loc.cit., p. 263
31. G. Tolkiehn, Diplomarbeit, University of Hamburg (1976)
32. Ch. Ackermann, R. Brodmann, U. Hahn, A.Suzuki, and G. Zimmerer, phys.stat.sol. (b) 74, 579 (1976)
Ch. Ackermann, R. Brodmann, G. Tolkiehn, G. Zimmerer, R. Haensel, and U. Hahn, J. Luminescence 12/13, 315 (1976)
33. U. Gerick, Diplomarbeit, University of Hamburg (1976)
34. H. Möller, R. Brodmann, U. Hahn, and G. Zimmerer, Solid State Commun. 20, 401 (1976)
35. E. Antoncik, Czech.J.Phys. B17, 953 (1967)
36. J.T. Devreese, A.B. Kunz, and T.C. Collins, Solid State Commun. 11, 673 (1972)
37. I.Ya. Fugol and A.G. Belov, Solid State Commun. 17, 1125 (1975)
38. T. Nanba, N. Nagasawa, and M. Ueta, J.Phys.Soc. Japan 37, 1031 (1974)
39. O. Chesnovsky, B. Raz, and J. Jortner, J.Chem.Phys. 57, 4628 (1972)
40. U. Hahn, B. Jordan, N. Schwentner, and G. Zimmerer, to be published

